Capturing the Reflectance Model of Soap Bubbles

Nigel Morris
nmorris@dgp.toronto.edu
University of Toronto

Abstract

We describe a system for rendering bubbles in natural environments using filtered environment maps. The system incorporates the optical properties of soap bubbles such as the interference patterns generated by the film. We describe a mathematical model to simulate the reflectance properties of the bubbles using a bi-directional reflectance field. This BRDF is used to filter an environment map captured from the desired location of the rendered bubble. We describe how to capture some of the model parameters from images.

1. Introduction

Soap bubbles have always been fascinating to children and scientists alike. Their iridescent reflections and minimalist form make them attractive toys and subjects for graphical simulation.

Studying the physical properties of individual bubbles and understanding the phenomenon associated with them is crucial to building realistic models of clusters of bubbles or foams. This project attempts to build a mathematical model that accurately simulates individual soap bubbles in a natural environment.

In recent years there have been several advances in simulating realistic-looking bubbles. Recently Keuck *et al*. developed a physically based foam simulation focusing on the physical forces between bubbles and simulating the lighting for clusters of bubbles [11]. Our approach focuses on a single bubble along the lines of Glassner's article on soap bubbles [6]. We attempt to match our rendered bubbles' appearance to photographs of bubbles in indoor and outdoor environments.

Most of our work revolves around developing a lighting model with BRDF filtered environment maps. Our work utilizes a long history of development of lighting reflectance models [1, 3, 12, 14, 15]. Extensive work has also been done in adapting BRDFs to environment maps [2, 5, 8, 10]. Recently Heidrich *et al*. described a method for rendering filtered environment maps at interactive frame rates [8]. The development of high speed environment maps was tangential to the aim of this paper so we used a naïve prefiltering process and leave the enhancements to future work.

2. Mathematical Model for Soap Bubbles

We attempted to develop a mathematical model of soap bubbles that closely approximates reality. The most striking aspects of soap bubbles are their reflective and refractive properties. Our research for the model concentrated on reproducing the interaction of light with the surface film of the bubbles and thus recreating the visual phenomena seen in reality.

2.1 Reflection

Initially we selected Ward's isotropic BRDF [15] model since it provides a true bi-directional reflective model and is thus more accurate than the Phong model. The model is not directly physically based but provides a decent approximation and is relatively easy to compute compared to more physically accurate models [1, 3]. Ward's model allows us to specify three parameters: diffuse (r_d), specular (r_s) and specular roughness (a):

$$L_i^r = f_r(\vec{w}_i \to \vec{w}_r) = \frac{r_d}{p} + r_s \frac{1}{\sqrt{\cos q_i \cos q_r}} \frac{\exp(-\tan^2(d)/a^2)}{4pa^2} \quad (1)$$

Equation (1) gives the reflected radiance (L) for a point i on an object's surface using Ward's BRDF, where q_r is the angle between the surface normal and viewing angle, q_i is the angle between the normal and the incident light, and d is the angle between the half-angle and the surface normal.

We can set up a scene and with a bubble with reflectance parameters and one light source. Then we can obtain the surface radiance at each point on the bubble's surface resulting from equation (1). We can then render

our image of the bubble by tracing a ray through the pixel and intersecting it with the front and rear bubble surfaces. So for each pixel *k*, the radiance is the sum of the contributing radiances along the ray (equation (2)). The pixel radiance will be a sum of the reflection from the front bubble film as well as the reflection from the light that reflects from the rear bubble film. The rear reflection will be slightly dimmer due to the light that is absorbed by the film (this is the *t* in equation (2)). We must also take into account the background intensity (I_b) for the ray that transmits through both films. This provides a decent approximation for an indoor scene with a point light source and an otherwise dark environment. This intensity for some viewing angle *r* is:

$$I^r = I_1^r + t^2 I_2^r + t^4 I_b^r \qquad (2)$$

It is a simple matter to generalize the model to work with multiple light sources; we would simply compute radiance for every light source and sum the resulting radiances to determine the brightness at *j*. Equation (3) shows the computation for *n* light sources.

$$I_j = \sum_1^n \left(\frac{r_d}{p} + r_s \frac{1}{\sqrt{\cos q_i \cos q_r}} \frac{\exp(-\tan^2(d)/a^2)}{4pa^2} \right) \qquad (3)$$

This model is still limited to a dark indoor environment, so we decided to develop a model that would be much more accurate for any environment. This was achieved by using environment maps. Basically an environment map is captured from the scene where a bubble is to be placed. This map is then projected onto the bubble and the bubble is rendered onto an image of the same scene without the environment map. This technique simply implements a Dirac-delta function where the light from the environment is reflected at one angle. The resulting images are closer to simulating an outdoor environment than before although we have lost the ability to define the surface roughness.

We can combine the properties of both environment mapping and the BRDF to obtain a good approximation for any lighting conditions. This is achieved by filtering every pixel in the environment map by the BRDF function and then applying the filtered environment map to the bubble surface.

The total reflected radiance for a solid viewing angle $\vec{w}_r$ in our filtered environment map is computed by integrating the incident radiance L^i over the incident hemisphere O_i [Glassner]:

$$L^r(\vec{w}_r) = \int_{\Omega_i} f_r(\vec{w}_i \to \vec{w}_r) L^i(\vec{w}_i) d\vec{w}_i^{\mathrm{N}} \qquad (4)$$

Where $f_r(\vec{w}_i \to \vec{w}_r)$ is the BRDF function relating incident light to the viewing angle and $d\vec{w}_i^{\mathrm{N}}$ is the projected differential solid angle. The projected differential solid angle represents the amount of energy that arrives from the incident light direction over the area covered by that pixel in the incident hemisphere. It is computed from the differential solid angle:

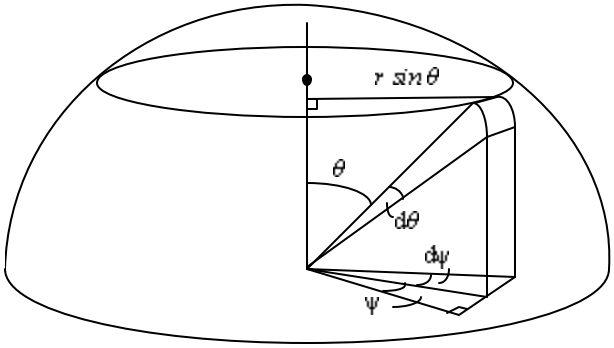

Figure 1. The solid angle $\vec{w}$ in the incident hemisphere

$$d\vec{w} = \frac{dA}{r^2} = \sin(q)\,dq\,dy$$

Then we can compute the projected differential area, and thus the projected differential solid angle:

$$dA^{\mathrm{N}} = r^2 \sin(q)\cos(q)\,dq\,dy$$
$$d\vec{w}^{\mathrm{N}} = \frac{dA^{\mathrm{N}}}{r^2} = \sin(q)\cos(q)\,dq\,dy \qquad (5)$$

Now we can completely express the reflected radiance function using equations (1), (4) and (5):

$$L^r(\vec{w}_r) = \int_{\Omega_i} \left(\frac{r_d}{p} + r_s \frac{1}{\sqrt{\cos q_i \cos q_r}} \right) \frac{\exp(-\tan^2(d)/a^2)}{4pa^2} L^i(\vec{w}_i)\sin(q_i)\cos(q_i)\,dq_i\,dy_i \qquad (7)$$

2.2 Interference

While capturing data samples it became apparent that bubble frequently exhibit iridescent rings and simulating this phenomenon would greatly enhance our model. The iridescence occurs when the soap film becomes thin enough for the reflection from the inside of the film to interfere with the primary reflection from the outside. White light is composed of light with wavelengths from ~380 to 780 nm and each wavelength corresponds to a different colour. The interference is dependent on the wavelength of the light, so certain wavelengths will be destructively interfered with while others will be constructively interfered with resulting in the iridescent display associated with bubbles.

2.3 Film Interference

In order to understand the mechanics of interference we need to look more closely at the interaction of light with the bubble film. A ray of light v strikes the outer surface of the film; a fraction t of the ray is transmitted and the rest (1-t) is reflected. Since the ray is traveling from a high speed medium (air) to a lower speed medium (soap film) the reflected ray v(1-t) undergoes a phase shift of p. The transmitted ray vt continues to travel through the soap film at a rate of c/n_g (where n_g is the index of refraction of the soap and c is the speed of light in air).

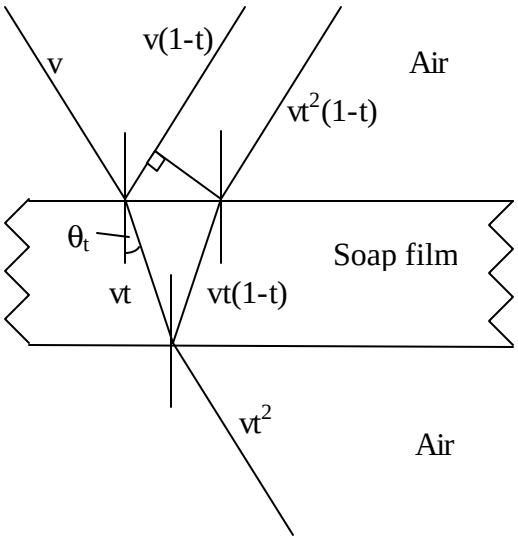

Figure 2: Light ray v interacts with the soap film and is reduced by the transmission fraction t when it is transmitted and is reduced by (1-t) when it is reflected.

The transmitted ray vt reflects on the interface between the soap film and the air inside the bubble. Part of the ray is transmitted as vt^2 and the rest is reflected as ray vt(1-t). The reflected ray once more hits the outer soap-air interface and is transmitted and reflected. We will ignore the reflected portion and its subsequent interactions. The final transmitted ray $vt(1-t)^2$ travels in a parallel direction to the initial reflection v(1-t) and causes interference.

We need to treat the rays as waves to understand interference. Thus, when the primary reflected wave overlaps with the secondary reflected wave we have interference. When the two waves are in phase we get constructive interference and when they are out of phase, destructive interference occurs. Thus the phase difference between the primary and secondary waves is what determines interference. In order to compute that we need to know the thickness of the soap film (d) and how many wavelengths (m) fit in the extra distance traveled by the secondary wave. Taking into account the phase shift of half a wavelength in the primary reflection, we can calculate the phase difference (d) as follows:

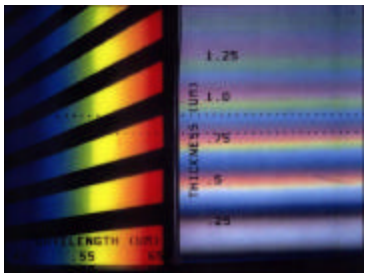

$$d = \frac{2p}{l}\left(2dn_g \cos q_t + l/2\right) \qquad (8)$$

Glassner derives an equation for the reflected intensity (I_r) from one soap film with interference [6]:

$$I_r = 4I_i R_f \cos^2(d/2) \qquad (9)$$

Remember that the secondary reflected light must be reduced by the transmission fraction squared. So the intensity of the reflected light (I^r) including interference and substituting our reflection function (L^r) is:

$$I^r = 4L^r(\vec{w}_r)\cos^2(d/2)t^2 \qquad (10)$$

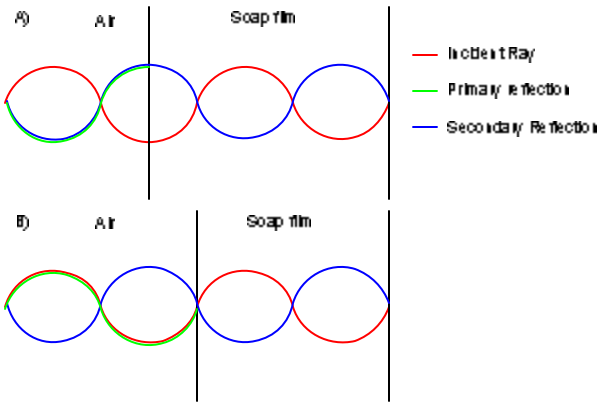

Figure 3: A) Demonstrates constructive interference – the secondary reflection matches the phase shifted primary reflection. B) Shows destructive interference with the secondary reflection out of phase of the shifted primary reflection.

Now we need to examine how white light behaves with interference. White light is composed of a multitude of rays with wavelengths from approximately 380 nm to 780 nm in the visible spectrum. Each wavelength corresponds to a colour in the spectrum. Since the wavelengths are different and according to equation (9), the amount of interference is dependent on wavelength, then some colours will be constructively interfered with while others are destructively interfered with. So, as the bubble thickness varies different colours are displayed resulting in the iridescent display seen in the data.

Another point to note is that colours are only observed when the bubble thickness is close to several wavelengths in thickness. Beyond this the bright fringes of interfered colours overlap giving white light again.

2.4 Curved Film Interference

In reality our bubble film is not flat, but curved so interference will not be exactly approximated by the above model. When the viewing angle gets steep the curved film will differ most from a flat one. What happens is the initial reflection will be at a different angle from the secondary reflection and interference should only occur when the waves are separated by less than their combined amplitudes.

Another effect of a curved film is the distance traveled by the ray producing the secondary reflection. When the viewing angle changes from zero, the distance traveled increases and thus the wavelengths that interfere will change. So there will be a spectrum of colour from the inside to the outside of the bubble assuming the bubble is thin enough.

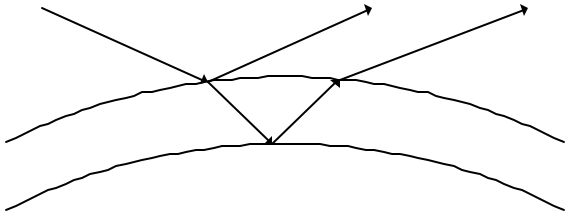

Figure 4: A curved film version of figure 2.

2.5 Putting it all together

Now we need to combine the environment map-BRDF model with the complete ray transmission model, taking into account both film interactions and the background intensity.

If we combine equation (2) with equation (10) we get the total intensity along a viewing direction *r*:

$$I^r = 4L_1^r(\vec{w}_r)\cos^2(d/2)t^2 + t^2(4L_2^r(\vec{w}_r)\cos^2(d/2)t^2) + t^4 L_b^r \qquad (11)$$

3. Implementation

3.1 Creating and Digitally Capturing Soap Bubbles

Soap bubbles are inherently difficult to observe due to their limited lifetime and fragile nature. A bubble mixture can be concocted from water, dish washing detergent and sugar. The sugar improves the surfactant strength and the lifetime of the bubble.

Bubbles are especially difficult to photograph out side, especially in windy conditions. We dis covered that a fixed focal length of approximately one metre allows the photographer get into position to capture a bubble most easily. Even so, many attempts are often required before a focused bubble can be captured.

An alternative method is to blow a bubble on to a dish where it can be easily photographed. The dish must be wet otherwise the bubble will burst upon contact. This method has several drawbacks: the dish itself enters into the reflections and specularities from the liquid on the dish will be observed if the azimuth is greater than zero. Also the liquid surface where the bubble connects to the liquid on the dish generates irregularities.

3.2 Environment Maps

We captured environment maps from a highly reflective silver coated glass bulb. The bulb was captured within target environment. Ideally the maps should have a high dynamic range so as to avoid data loss. This is especially important for the specular highlights, since most cameras will automatically attempt to balance the brightness of the scene. The bubble has much less specular reflectance than the glass bulb, so the environment map must capture the relative brightness of the sky or lamps compared to the rest of the scene. Using high dynamic range maps went beyond the scope of this project so exposure control was used to avoid saturating the bright spots.

Notice that the equation (7) to compute the BRDF requires integration over the whole incident hemisphere. We can discretize this integral into a summation over the pixels in the hemisphere and their corresponding solid angles:

$$L^r(\vec{w}_r) = \sum_{\Omega_i} \left(\frac{r_d}{p} + r_s \frac{1}{\sqrt{\cos q_i \cos q_r}} \frac{\exp(-\tan^2(d)/a^2)}{4pa^2} L^i(\vec{w}_i) \sin(q_i)\cos(q_i) dq_i dy_i \right) \quad (12)$$

In fact, the BRDF is largely directional with most of the intensity clustered around the reflection of the viewing angle. This allows us to approximate the incident hemisphere by a window around the reflected viewing angle:

$$L^r(\vec{w}_r) = \sum_{W_i} \left(\frac{r_d}{p} + r_s \frac{1}{\sqrt{\cos q_i \cos q_r}} \frac{\exp(-\tan^2(d)/a^2)}{4pa^2} L^i(\vec{w}_i) \sin(q_i)\cos(q_i) dq_i dy_i \right) \quad (13)$$

The window size is in fact a function of the Gaussian roughness a. Currently we have not intergrated this function into our system, rather the user manually adjusts the window size. This approach works if the diffuse component is negligible since the diffuse lighting outside of the window is lost. A better approach than a window is to use mipmaps of the environment map, using the lowest detail maps furthest from the centre reflected viewing angle and increasing the mipmap detail as the specular component increases as described in [10].

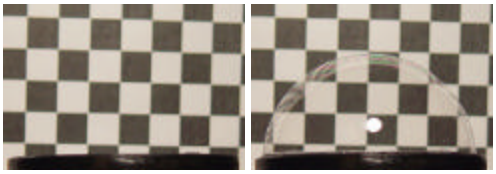

Figure 5: The two images used to capture the transmission fraction of the bubble.

3.3 Model Parameters

The transmission fraction t was empirically found by photographing a bubble on a matte black dish inside of a matte black box with a checkered background. The box blocked out most of the specular reflections so that the transmission could be determined, and the bubble was captured at zero azimuth to avoid reflections from the dish. Two photographs were taken from the same fixed camera, one with a bubble in place and one without. The difference between the photos was used to compute the transmission fraction. In this case the fraction to the power of four since the light passes through the soap film-air interface four times.

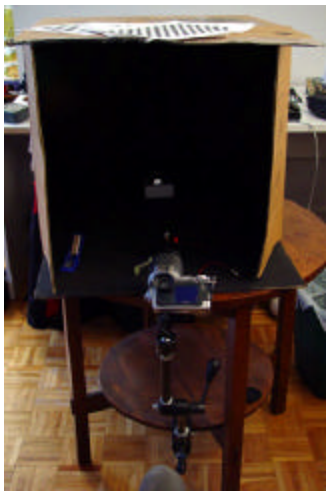

Figure 6: Apparatus used for bubble capture

By conservation of energy the reflected light can be determined from the transmission fraction. This means the combined diffuse and specular reflective components must be (1-t), so:

$$r_d + r_s = 1 - t \quad (14)$$

Our implementation allows the user to use our determined transmission fraction and supply a ratio (f) between the specular and diffuse components.

Alternatively the user may specify RGB values for all three. The implementation also allows the user to specify the roughness coefficient.

We used a refractive index of 1.4 for the soap film.

3.4 Interference Implementation

In order to implement the interference model described in this paper it was necessary to map wavelengths to RGB intensities. This was accomplished by converting wavelengths into the CIE colour space and then mapping to the RGB space, clamping when necessary. We modified a system by Walker to achieve this [16].

Initially a small set of ten samples in the spectrum where taken and interference patterns were observed. A problem occurred when the soap film thickness was increased to a point where the interference patterns all overlapped. There were points where the sample set still converged and bands were produced. This continued to be observed when thirty samples were used. One hundred samples adequately covered the spectrum leaving no visible banding.

4. Results

We present some results with various roughness settings (a) and soap film thickness (d) and diffuse-specular ratios (f). Pictured below is a small real bubble to the left with our larger rendered bubble using an environment map that does not exactly match but gives a decent approximation of the location.

Figure 8: The environment map used for the bubbles in Figure 7. This map is less than perfect due to the reflected protrusion of at the top. This artifact is noticeable in the rendered bubbles.

Several factors reduce the realism of the bubbles in the results. We believe a better model of the Fresnel effects near the edge of the bubbles would improve some of the reflections. Compare the edges of the real bubble with the rendered bubble in figure 7. Also the bubble environment map is from the same location but a different angle. There is a noticeable tree in the reflection of the environment map but not so in the real bubble. Also as mentioned in figure 8, the top of the bulb does not reflect the sky as it should.

Figure 9 shows some examples of real interference in the small bubble to the right along with our simulated bubble with varying film thicknesses (d). The interference tends to brighten the bubble significantly – reducing the realism when compared to similar real bubbles. Although the first image in figure 9 simulates the interfering colours in the real bubble almost exactly.

Another set of results is displayed in figures 10-13. The location was in an alley with snow on the ground. In this set we obtained good environment maps by locking the exposure settings of the camera to the sky. Also the reflective ball was balanced on a stand and the reflections were very close to those experienced by the real bubbles. Figure 14 shows the filtered environment maps used.

a) 
b) 
c) 
d) 

Figure 7: a) Bubble rendered with a=0.01 and f = 0.3
b) Bubble rendered with a=0.02 and f=0.3
c)&d) The corresponding filtered environment maps for the bubbles.

Figure 9: From left to right, d = 260, 460, 860, 1660, 3260 nm

5. Future Work

The film thickness could be animated to simulate the gravitational effect of drainage in the bubbles. This would generate the characteristic interference bands seen at the top of bubbles – since their tops would become thinner as drainage occurs.

As mentioned in the introduction, adapting the model described in this research to an interactive version would be a natural progression of the work. Implementing the hierarchical BRDF filtering as described in Kautz et al. [10] and Hiedrich et al. [8] could readily be achieved.

The reflection realism itself could potentially be improved in several ways. Incorporating high dynamic range maps [4] into the system would provide much better scene intensity information which would translate to better environment maps. Another improvement would be to adapt a physically based BRDF to the model. The Cook-Torrance [3] model could be so used. An alternative approach might be to use spherical harmonics to capture the lighting model of bubble as described by Ramamoorthi et al. [13].

The technique described in this research could be further generalized to other transmissive specular objects. This approach could potentially be combined with environment matting by Zongker [17].

6. Conclusion

We have presented a system which utilizes a BRDF to filter the environment of a bubble and incorporates optical properties of the bubble. The results give decent approximations of bubbles in natural environments. The quality of the results seems to depend greatly on the environment map itself. If a good environment map is obtained without saturated bright spots, a good reflection model for the bubble can be obtained.

7. References

[1] P. Beckmann, and A. Spizzochino, "The Scattering of Electromagnetic Waves from Rough Surfaces", Artech House, Norwood, 1987.

[2] B. Cabral, M. Olano, and P. Nemec, "Reflection space image based rendering". In *Computer Graphics* (SIGGRAPH '99 Proceedings), August 1999.

[3] R. L. Cook, and K. E. Torrance, "A reflectance model for computer graphics". *ACM Transactions on Graphics*, 5(1):51--72, 1982.

[4] P. E. Debevec, and J. Malik, "Recovering high dynamic range radiance maps from photographs". In *SIGGRAPH 97* (August 1997), pp. 369--378.

[5] P. Debevec, T. Hawkins, C. Tchou, H.-P. Duiker, W. Sarokin, and M. Sagar, "Acquiring the reflectance field of a human face", *Computer Graphics* (SIGGRAPH), 2000.

[6] A. S. Glassner, "Soap Bubbles", *IEEE Computer Graphics and Applications*, 20(6):99--109. 2000.

[7] A. S. Glassner, *Principles of Image Synthesis*. Morgan-Kaufman, 1994.

[8] W. Heidrich and H.-P. Seidel, "Realistic, hardware-accelerated shading and lighting", In *SIGGRAPH '99 Proceedings*, August 1999.

[9] D. S. Immel, M. F. Cohen, and D. P. Greenberg, "A radiosity method for non-diffuse environments", In *Proceedings of SIGGRAPH '86*, pages 133--142. ACM, New York, 1986.

[10] J. Kautz, P. Vazquez, W. Heidrich, and HP. Seidel, "A Unified Approach to Prefiltered Environment Maps", In *Eurographics Rendering Workshop*, 2000.

[11] H. Kueck , C. Vogelgsang , and G. Greiner, "Simulation and Rendering of Liquid Foams". *Proc. Graphics Interface* pp 81--88, 2002.

[12] S. K. Nayar, K. Ikeuchi, and T. Kanade, "Surface reflection: Physical and geometrical perspectives", *IEEE Trans. Patt. Anal. Mach. Intell.*, 13(7):611--634, July 1991.

[13] R. Ramamoorthi and P. Hanrahan, "A signal-processing framework for inverse rendering", *Computer Graphics* (SIGGRAPH), 2001.

[14] K. E. Torrance and E. M. Sparrow, "Theory for Off-Specular Reflection from Roughened Surfaces", *Journal of the Optical Society of America*, 57(9):1105--1114, 1967.

[15] G. J. Ward, "Measuring and modeling anisotropic reflection", In *Proceedings of SIGGRAPH '92*, pages 265--273. ACM, New York, 1992.

[16] J. Walker, "Colour Rendering of Spectra", Available: http://www.fourmilab.ch/documents/specrend/, April 1996.

[17] D. E. Zongker, D. M. Werner, B. Curless, D. H. Salesin, "Environment Matting and Compositing", *Proc. ACM SIGGRAPH*, 1999.

Figure 10: Rendered bubble i) bottom left

Figure 11: Rendered bubble i) left

Figure 12: Rendered bubble i) left

Figure 13: Rendered bubble ii) right

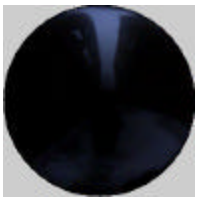

Figure 14: Filter map for bubble i) left
Filter map for bubble ii) right

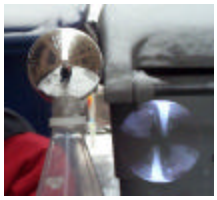

Figure 15: Environment maps used above